

References and Notes

1. A. Kvale, *Norsk Geol. Tidsskr.* **25**, 193 (1945).
2. N. L. Carter, J. M. Christie, D. T. Griggs, *J. Geol.* **72**, 687 (1964); C. B. Raleigh, *ibid.* **73**, 369 (1965); D. T. Griggs, J. S. Starkey, H. W. Green, J. D. Blacic, D. W. Baker, N. L. Carter, J. M. Christie, *Trans. Amer. Geophys. Union* **46**, 541 (1965); B. E. Hobbs, *ibid.* **47**, 494 (1966).
3. H. W. Green, *Trans. Amer. Geophys. Union* **47**, 491 (1966).
4. D. W. Baker, H. R. Wenk, J. M. Christie, in preparation.
5. D. W. Baker, *Trans. Amer. Geophys. Union* **46**, 541 (1965); unpublished results.
6. H. R. Wenk, D. W. Baker, D. T. Griggs, *Science*, this issue.
7. C. S. Barrett and T. B. Massalski, *Structure of Metals*, (McGraw-Hill, New York, ed. 3, 1966), pp. 555-56; 570-72; 579-83.
8. H. Hu and S. R. Goodman, *Trans. Met. Soc. AIME* **227**, 627 (1963).
9. P. A. Beck, *Trans. AIME* **191**, 474 (1951); *ibid.*, p. 475; T. J. Koppenaal, M. N. Parthasarathi, P. A. Beck, *ibid.* **218**, 98 (1960).
10. R. K. McGeary and B. Lustman, *J. Metals* **3**, 994 (1951).
11. Publication No. 594 of the Institute of Geophysics and Planetary Physics. Supported by NSF grant GP5575. B. E. Hobbs' work on deformation and annealing of single crystals of quartz provided inspiration for these experiments. D. T. Griggs and J. M. Christie provided laboratory facilities and helpful discussion. Correspondence with Hsun Hu was stimulating. J. de Grosse prepared the thin sections.

26 June 1967

X-Ray Fabric Analysis of Hot-Worked and Annealed Flint

Abstract. *Two specimens of flint described by Green have been subjected to intensive x-ray fabric analysis. The specimen compressed in the β -quartz field recrystallized to a fabric with a strong maximum of c-axes parallel to the direction of compression and a weaker equatorial concentration perpendicular to the axis of compression. Annealing of a similar specimen eliminated the equatorial concentration and strengthened the axial concentration six- to eightfold. In the latter specimen, the fabric determined by x-ray analysis agrees closely with Green's optically measured fabric. It is possible to obtain c-axis fabrics directly from the very weak 0003 diffraction peak.*

Green discovered that an extremely strong preferred orientation developed a hot-compressed specimen (DT-460) of Dover flint when it was annealed (1). A similar specimen (DT-459) without annealing appeared optically to have a much weaker orientation in the same direction, but the grain-size was so small that universal-stage fabric measurement was impossible. We here give the x-ray fabric data of the fine-grained hot-worked sample, and verify Green's optically determined fabric of the annealed sample.

A modified Philips pole-figure goniometer and diffractometer were used to obtain transmission intensity profiles of suitable diffracting planes in a section 90 μ thick, cut parallel to the direction of compression, and rotated in its own plane. The deformation of the specimens was axially symmetric. Other similarly deformed specimens have exhibited a fabric with axial symmetry. For such a specimen transmission profiles are sufficient to characterize the fabric. Since the specimen is only rotated in its own plane, no absorption correction is necessary. In our case profiles extending from parallel to perpendicular to the compression axis have been used. The large grain-size (~ 0.03 mm) of the annealed specimen required a further modification of the Philips device to obtain adequate counting statistics. The specimen was rela-

tively rapidly oscillated $\pm 5^\circ$ about the normal to the plane of the primary beam and to the counter; this procedure provided an integration over lattice planes that are within 5° of being at right angles to the section. The usual method of integration by translating the specimen in its own plane was precluded by the small size of the

highly oriented region in the specimen, which was not larger than the beam size (diameter, 1 mm). Oscillation or translation modifications are necessary as soon as there are less than 5000 to 10,000 grains in the irradiated area.

A number of profiles have been measured in both specimens (DT-459: $10\bar{1}0$, $20\bar{2}1$, $10\bar{1}1$, $10\bar{1}2$, $10\bar{1}4$, $11\bar{2}0$, $11\bar{2}1$, $11\bar{2}2$, $11\bar{2}3$, $21\bar{3}1$; DT-460: $20\bar{2}0$, $20\bar{2}1$, $20\bar{2}2$, $11\bar{2}0$, $11\bar{2}2$). Three profiles for DT-459 are shown in Fig. 1. Because of the low intensity of the basal 0003 reflection and its close proximity to the much stronger 1122 reflection as shown in the powder pattern of Fig. 2a, it has not hitherto been possible to isolate the 0003 peak sufficiently to permit determination of an 0003 pole-figure. The very strong preferred orientation of DT-460 indicated that if the plane normal to the c-axis concentration were set at the critical Bragg angle, the 0003 peak would be more intense than the 1122 peak. This was found to be the case (Fig. 2b). The use of a fine receiving slit on the counter, and careful alignment of the collimator system permitted almost total isolation of the 0003 peak, so that it was possible to measure 0003 profiles in both DT-460 and in DT-459 (Fig. 3). The background in these profiles away from the c-axis maxima is mostly instrumental noise. Better electronic circuits are now available than the one we used, so that

Table 1. Measured values of I , I° , and ρ_2 and calculated c-axis concentrations parallel to the compression.

Specimen	hkl	Relative intensities corrected for background		Concentration given as multiples of uniform distribution	
		I at σ_1	I° random	ρ (hkl)	ρ (0001)
DT-459	$11\bar{2}2$	22	110	.40	7.2
	0003	9	2.5	(4.8)	
DT-460	$11\bar{2}0$	11	71	.74	47.8
	2020	6	48	.45	36.0
	2021	4	30	.50	37.5
	1122	4	101	.16	44.0
	0003	25	2.5	(73.0)	
	2022	2	32	.22	35.2

Table 2. The c-axis concentrations parallel to compression given as multiples of uniform distribution.

Specimen	Optical (U-stage)	X-ray peak-intensity ratio	Inverse pole figure	Normalized c-axis profile
DT-459		7.2	7.0	4.8
DT-460	107*	40	46	73

* Only larger grains measured (~ 0.03 mm).

we believe it will be possible to detect variations in c -axis orientation which depart from uniform distribution by as little as 50 percent. To our knowledge, this is the first time that the c -axis

fabric has been measured directly by x-ray techniques.

The concentration of poles $\rho(\phi)$ for an axially symmetric fabric, expressed as multiples of uniform dis-

tribution, is given by the formula:

$$\rho(\phi) = \frac{I(\phi)}{\int_0^{\pi/2} I(\phi) \sin \phi d\phi} \quad (1)$$

where ϕ is the angle between a pole and the compression axis and $I(\phi)$ is the measured intensity corrected for background. It can be seen that, when this formula is applied for the c -axis profile with a single maximum in the direction of compression, small errors in the background cause large errors in the maximum concentration. This is because the peak occurs where the area factor, $\sin \phi$, is zero. Another method of obtaining the c -axis concentration parallel to the compression axis is more accurate. The peak intensities I_1 and I_2 of two planes hkl at a point in the pole figure are proportional to the peak intensities I_1° and I_2° of the same planes in a randomly oriented specimen multiplied by their respective concentrations ρ_1 and ρ_2 at that point.

$$\frac{I_1}{I_2} = \frac{I_1^\circ \rho_1}{I_2^\circ \rho_2} \quad (2)$$

The relative intensities are taken from 2θ profiles over the two peaks on the sample (I_1, I_2) and on a powder specimen (I_1°, I_2°) with the same geometry (Fig. 2). The concentration ρ_2 is obtained by normalizing the profile of hkl according to Eq. 1. The results using this method to determine the c -axis concentration (ρ_1) parallel to the compression are listed in Table 1.

The c -axis profiles and the inverse

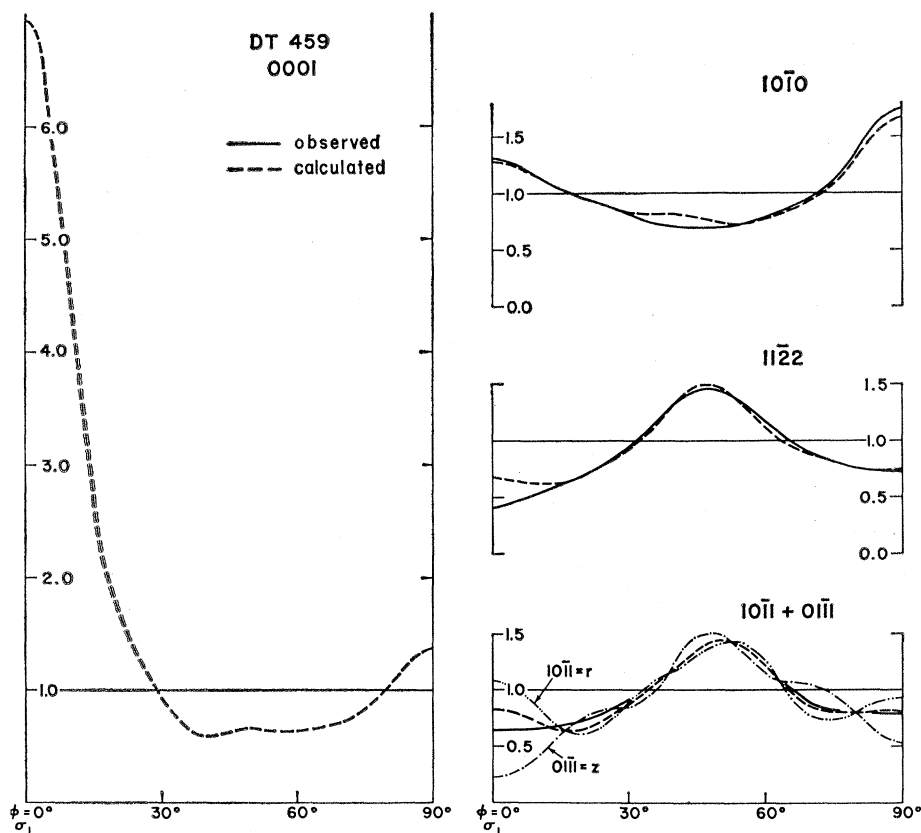


Fig. 1. Measured transmission profiles for various planes in DT-459 (solid) and calculated profiles (dashed) on the assumption of trigonal symmetry. Intensities of the ordinate are multiples of uniform distribution. The angle ϕ is measured from the pole of the reflecting plane to the direction of compression (σ_1). Note that the two unit rhombohedrons $r = 1011$ and $z = 0111$ have a similar distribution, although the poles of r tend to have a secondary maximum and those of z a minimum parallel to the direction of compression.

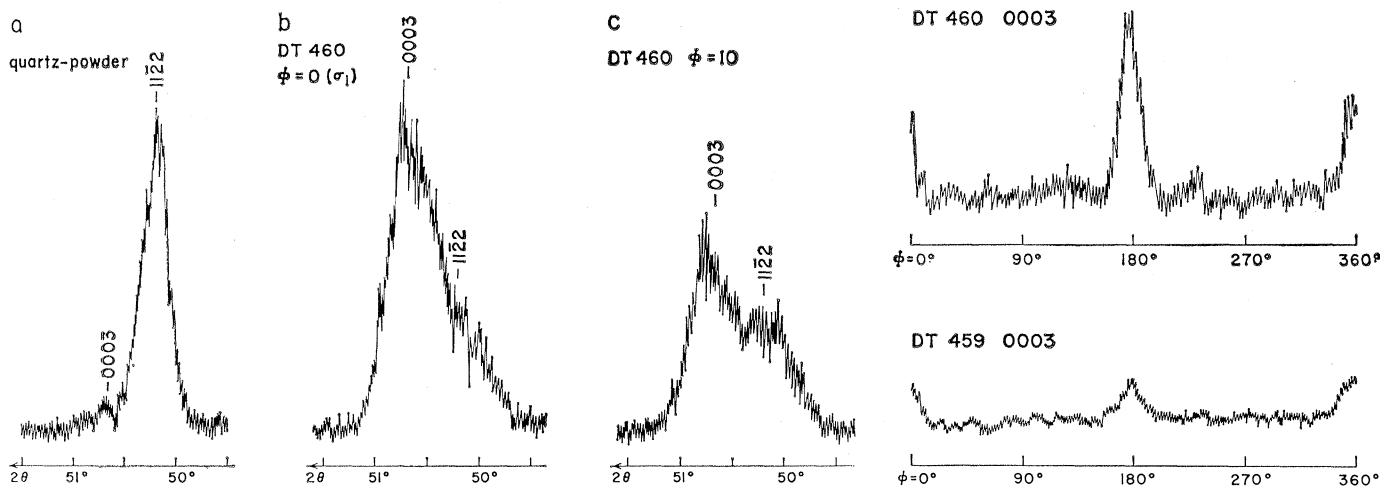


Fig. 2 (left). The 2θ profiles with small counter receiving slit, taken with a Philips pole-figure goniometer. Ordinate: relative intensity; abscissa: 2θ angle. (a) Quartz powder with random orientation. The peak-height ratio 1122/0003 is 44. (b) $\phi = 0^\circ$. Note that in this position the 0003 reflection is much stronger than 1122. (c) $\phi = 10^\circ$. The 0003 peak decreases rapidly in departing from the $\phi = 0^\circ$ position. Fig. 3 (right). Measured 0003 transmission profiles of DT-460 and DT-459. Ordinate: relative intensity; abscissa: angle to direction of compression, ϕ . The background is mostly instrumental noise and not a contribution from randomly oriented grains.

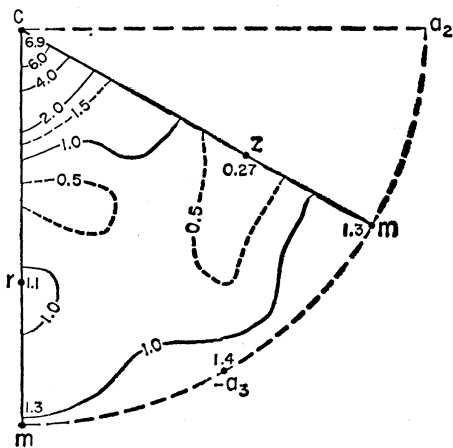


Fig. 4. Inverse pole-figure (equal area projection) of DT-459 showing the distribution of the compression axis with respect to crystal coordinates. Calculated from ten observed profiles with 16th order harmonics; (r is the strong, z the weak reflecting unit rhombodron).

pole-figure were indirectly obtained by using Roe's method for spherical harmonic analysis of fabric data (2). The adaptation of this method to the trigonal symmetry of quartz and its application to the determination of quartz fabrics are described in detail elsewhere (3). The inverse pole-figure of DT-459 (Fig. 4) was deduced using 16th order Legendre polynomials, and several profiles have been calculated which compare satisfactorily with the observed data (Fig. 1). The main feature of the inverse pole-figure of DT-459 is a strong maximum of compression axes parallel to the c -axis (7 times uniform distribution). A secondary concentration of compression axes is in the zone of the prisms (1.5 times uniform distribution). Unlike specimens deformed in the α -field (3), in this specimen deformed in the β -field there is no significant tendency for other crystallographic directions to have additional preferred orientation. In DT-460 the high concentrations necessitated high-order spherical harmonics to represent the steep topography. With the limited data available, the serious termination errors in these high-order harmonic calculations were reduced using hexagonal symmetry, but still produced artificial secondary features. The c -axis maximum in the direction of compression was determined with 20th order harmonics to be 46 times uniform distribution.

Annealing thus increased the strength of the c -axis maximum six- to eightfold and obliterated the concentration of c -axes perpendicular to the compression. Green (1) has determined

the concentration of c -axes in DT-460 optically (U-stage). His results are compared in Table 2 with the x-ray data obtained from different methods. Within the range of experimental errors there is agreement between the different data. The x-ray values for DT-460 have to be regarded as a lower limit because the beam-size is slightly larger than the highly oriented area and minute disalignments bring this area out of the focus. In the optical analysis only the larger grains (~ 0.03 mm) were measured, whereas by the x-ray technique the orientation of all grains is recorded. Green estimates that the small grains are less well oriented, and that their inclusion could reduce the concentration by as much as a factor of 2.

The fact that c -axis fabrics of quartz have been directly measured by x-rays offers new opportunities in structural petrology. It appears that presently available improved diffractometers are sufficiently better than ours to permit the direct measurement of c -axis fabrics in fine-grained quartz rocks with as much sensitivity as optical techniques.

H. R. WENK
D. W. BAKER
D. T. GRIGGS

Institute of Geophysics and Planetary Physics, University of California, Los Angeles

References and Notes

1. H. W. Green, *Science*, this issue.
2. R. J. Roe, *J. Appl. Phys.* **36**, 2024 (1965).
3. D. W. Baker, H. R. Wenk, J. M. Christie, in preparation.
4. Publication No. 603 of the Institute of Geophysics and Planetary Physics. Supported by NSF grant GP5575. We thank J. M. Christie for discussion and Van Waters and Rogers, Inc. for the loan of a Philips goniometer.

26 June 1967

Brown and White Fats: Development in the Hamster

Abstract. Sites occupied by multilocular brown fat in the adult hamster are occupied by unilocular cells in very young animals. Immature brown fat cells are laid down in the unilocular cell matrix at 3 to 5 days of age. White fat in the hamster does not develop from cells closely resembling mature brown fat.

Recent demonstrations of the thermogenic function of brown fat (1) have led to renewed interest in this tissue. An unanswered question is its

relationship to white fat. Mature brown-fat cells appear histologically similar to multilocular cells found in developing white fat in such animals as rabbits and mice. This similarity has led to the suggestion that brown fat may be identical, or closely related, to immature white fat (2). However, recent investigations of the two types of multilocular cells with the electron microscope have indicated that some differences exist (3). The differences are well discussed in a recent review (4). We present further evidence, based upon light-microscopic investigations, that brown fat is not identical to developing white fat in the hamster. Furthermore, unilocular cells are formed several days before the appearance of multilocular cells.

In the adult hamster the subscapular region is occupied by brown fat, while the inguinal region has white fat. We have studied the development of adipose tissue in these regions as examples of the development of brown fat and white fat, respectively, and have then compared the processes in the two sites.

The animals studied ranged from the 12-day fetus, through newborn to animals 30 days old. They were obtained from adults maintained on a 12-hour light cycle with unlimited access to food and water (5). Tissues from both sites were removed from animals of known age, fixed in 10 percent formalin or Bouin's fixative, and appropriately processed for staining in Mallory's triple stain, hematoxylin and eosin, Oil Red O, or Sudan III. Fetal animals were usually studied in whole-body serial sections.

No evidence of multilocularity has been seen in presumptive subscapular adipose cells in the fetal hamster, but occasional unilocular cells were observed. The cell type which will give rise to the unilocular cells of the subscapular deposits becomes visible at about 12 days of gestation. These precursor cells are numerous by 13 days and are seen as cellular deposits in the intermuscular connective tissue of the subscapular region. In the 14- and 15-day fetus the deposits increase in size, with little evidence of other specialization. Parturition occurs during the 15th day of gestation.

At 1 to 2 days of age, a light-colored tissue deposit is grossly visible in the subscapular region. Histological study reveals the same appearance as described for the 13- to 15-day fetus, except the cells are more